Above-100 GHz Wave Propagation Studies in the European Project Hexa-X for 6G Channel Modelling

Pekka Kyösti*‡, Katsuyuki Haneda†, Jean-Marc Conrat§, Aarno Pärssinen*
*Centre for Wireless Communications, University of Oulu,
†Aalto University School of Electrical Engineering, Finland
‡Keysight Technologies, Oulu, Finland
§Wireless Engineering and Propagation, Orange Labs, Belfort, France

***Abstract*—We describe capabilities and plans to characterize above 100 GHz radio channel and propagation effects as part of a 6G research project Hexa-X. The starting point is the existing knowledge of radio propagation gathered by prior measurement and theoretical studies. Then we define measurement equipment, planned or performed campaigns, and discuss some challenges related to measurements at upper mm-wave frequencies. For several reasons the channel measurements are more time consuming on higher frequencies and it is not easy to collect enough data for statistical analysis. Hence we briefly introduce a stored channel model that will be developed based on the gathered channel measurement data. This initial channel model can be used as it is for physical layer studies through simulations and also as a basis for future channel models.**

Keywords*—Propagation, measurements, terahertz, channel modelling.

I. Introduction

Research on the field of telecommunications is moving towards sixth generation (6G) as the fifth generation (5G) networks and terminals are maturing to the commercial phase [1]. European research project Hexa-X started at the beginning of year 2021. Among other targets, it will study network, communications, and hardware technologies for achieving extreme data rate and extreme capacity. Hexa-X is one of the European research projects aiming at developing key technologies of future generation wireless systems, similarly to the IST-METIS and IST-WINNER, that investigated the same for 5G and 4G systems, respectively.

The target peak data rate of a single link is set to 100...1000 Gbps depending on the most data intensive use cases defined in the project. Since the spectral efficiency cannot be increased endlessly, it is evident that extremely wide bandwidths are needed to reach the target. This turns the interest towards upper millimetre wave (mm-wave) and THz frequencies, i.e., towards 100–300 GHz and above 300 GHz spectrum. Current lower mm-wave frequencies of 5G systems do not provide enough free spectrum for 6G needs. Utilization of above 100 GHz radio spectrum for communications, positioning, imaging, and sensing purposes provides many practical challenges. A major difficulty is the compensation of very high propagation losses inherent to the use of higher frequency band. This necessitates, e.g., beyond state-of-the-art power generation capability by radio frequency (RF) components, high gain antennas, and very elaborated beamforming and beam allocation techniques.

Radio channel is the key component in wireless communications and all other mentioned uses of RF devices. Understanding of radio channel characteristics at upper mm-wave and THz frequencies is important in the first place to identify feasible applications depending on the frequency bands. This information can be used to set research focus and targets for different frequency bands. Radio propagation and channel models are needed for assessing, e.g., possible link distances, required antenna gains, and supported mobility schemes. In a later phase channel models are to be used for evaluating performances of communication, imaging, and positioning schemes by simulations. One of the targets is to enable co-simulation with as realistic hardware (HW) performance models as possible to study future communications systems as examplified in [2]. Finally, when HW prototypes and first products are manufactured, they can be tested against channel conditions that are defined by the channel models and generated by test equipment, such as fading emulators.

The primary method of channel characterization is measurement of received power or transfer functions with different measurement antennas and equipment. On lower frequencies, especially below 6 GHz RF, dedicated channel sounders were often used. Sounding signals were either temporally short impulses, spread spectrum signals, or frequency sweeping tones. In general, the channel sounding typically becomes more challenging as the frequency increases due to the need of wider bandwidth and beamforming options, imposing hardware challenges to analog-to-digital converters and radio frequency component designs such as electrical beamforming antennas. Currently few sophisticated channel sounders are available for above-100 GHz, though they still do not allow real-time, time-varying directional channel sounding due to the need of *mechanically* scanning fixed-beam directional antennas, e.g., a horn antenna, over angles. For above-100 GHz RF, the sounding may be more conveniently performed with commercial measurement equipment, such as network analyzers. As a result, versatile database of at above 100 GHz radio channels is yet to be developed such that the extent of database becomes as large as those at below 6 GHz for 4G investigations. The use of digitizing revolution, i.e., deep learning, is not possible without such a large database. Collective efforts to measure *and share* the data are essential.

In this paper we sketch the current knowledge of above 100 GHz propagation characteristics and reveal some obvious knowledge gaps. We also discuss our approaches to channel modelling for 6G, which needs to cover the mentioned frequency range.

II. Review of existing knowledge about above-100 GHz radio channels

This section summarizes insights about above-100 GHz wave propagation according to previous measurement campaigns reported in the literature in terms of 1) wave-material interaction, 2) atmospheric losses and 3) multipath characteristics.

A. Wave–material interaction

The most widely referenced source of wave-material interaction for radio waves would be the ITU-R recommendation P.2040 [3]. It specifies insulating and conducting parameters for various materials in our living space up to 100 GHz RF in the best case, but lacks those for above 100 GHz RF. Measurements that would complement this lack of parameters are summarized as follows.

1) Reflection and scattering: Reflections from plasterboard and wall papers are analyzed in [4], [5] between 100 GHz and 1 THz with the effects of surface roughness. Due to comparable roughness of surfaces with the wavelength at above-100 GHz, scattering is more pronounced than below-100 GHz RF. Analyses of scattering from, e.g., a plaster and wall paper, show that the Kirchhoff theory and existing mathematical model of directive scattering describes the measurements well [6], [7]. Man-made metallic surfaces with controlled roughness are used to observe the scattered fields from 100 to 400 GHz RF, showing the effects of correlation length and heights of the roughness on the wave scattering pattern across observation angles [8].

2) Penetration: Increased penetration losses for higher RF up to 10 THz are reported for commonly-found materials in our living spaces in [5], [7], [9]–[12]. Estimated refractive indices on the other hand show constant values between 100 GHz and 1 THz [5], [13].

3) Radar cross section: Radar cross sections are reported for human bodies at 140 and 220 GHz, revealing the greater cross section as the frequency increases [14].

B. Atmospheric losses

Free space path loss is needed, e.g., for link distance consideration. In terrestrial communications the atmospheric attenuation affects the distance dependent path loss. At lower frequencies the effect is negligible, but at upper mm-wave and THz frequencies the impact must be at least considered. Main mechanisms of the atmospheric attenuation are the molecular absorption and the specific attenuation due to rain and fog. The latter naturally takes place mainly in outdoor scenarios, but the first one affects also indoor transmission. In both cases the attenuation can be modelled as a linear function in decibel units, i.e., in dB/km units.

The molecular absorption is caused mainly by different isotopes of water molecules in water vapour. This interaction causes strongly frequency dependent absorption of radio waves, which is observed as an absorption spectrum with certain spectral lines [15]. Beer-Lambert's law can be used for modelling the molecular absorption as described in [16]. It is affected by the density and the absorption cross section of molecules, which depends in the water vapour case on the temperature, humidity and operating frequency. There are no strong absorption lines on frequencies between 100 and 300 GHz and in typical conditions the attenuation varies between 0.15 and 30 dB/km having the strongest peak at 183 GHz.

Additional attenuation can be experienced in outdoor links in heavy rain conditions. The specific attenuation due to rain depends on the rain rate, measured in mm/h units. In light to violent rain, i.e., in 1 to 50 mm/h rain rate, the attenuation varies between 1 and 17 dB/km on 100 to 300 GHz frequency. The attenuation is highest around 120 GHz frequency. ITU-R P.838-05 specifies the rain attenuation up to 1 THz frequency in [17]. Fog and cloud attenuation are specified in ITU-R P.840-17 [18] up to 200 GHz.

C. Multipath characteristics

The following summarizes classifications and findings in existing papers [19]–[34] reporting multipath wave propagation for above-100 GHz based on channel sounding.

1) Application scenarios: Most papers cover short-range indoor links up to 50 m of distance, including laboratory and office [19]–[22], [24], [25], [31], [33], large halls such as shopping mall and airport [23], [34], data center [26], [29], [30], [35], desktop [19], [36] and train-to-infrastructure communications [27] scenarios. Only one paper [37] reports outdoor urban channel sounding of link distance up to 100 m.

2) Pathloss: Pathloss models cover 140 GHz [20], [22], [23], [25], [32]–[34], [37], 190 GHz [31] and 300 GHz [19], [22], [24], [26], [27], [29], [30], [35], [36] RF. As most measurements cover links with line of sight (LOS), their pathloss models are similar to the free-space formula where the pathloss exponent is close to 2. The pathloss exponent in non-line of sight (NLOS) indoor office scenario is 2.8 according to [33]. Pathloss models, in many cases called *omni-directional* pathloss models, are independent of antenna gains at link ends. Raw channel sounding data, e.g., channel impulse responses, implicitly include the antenna effects. Proper de-embedding of antenna gains from measurements requires three-dimensional double-directional measurements such as the one presented in [31], [33]. Otherwise the reported pathloss model may have ambiguity in terms of the reference pathloss, e.g., at 1 m link distance, due to improper de-embedding of antenna gains.

3) Delay and angular spreads: Measurements of indoor office omni-directional channels show root mean squared (RMS) delay spread up to 20 ns, but mostly smaller than 10 ns [25], [31], [33], while it is reduced to 1 ns at 300 GHz according to a data center environment [30]. In a large indoor hotspot, like an airport check-in hall, much greater delay spread up to 120 ns are reported [34]. Some papers [20], [29] report the coherence bandwidth instead of the delay spread as a relevant metric to multi-carrier transmission such as orthogonal frequency division multiplexing (OFDM). Both D-band laboratory and 300 GHz data center channels show the coherence bandwidth around 1 GHz.

Angular spread may be indicative for antenna correlation when link ends have arrays with multiple RF chains and hence allow spatial multiplexing similarly to legacy Multiple-Input-Multiple-Output (MIMO) radios. Indoor omni-directional channel measurements report mostly up to 50°

and 10° azimuth and elevation spreads [31], [33], [34], but sometimes up to 70° azimuth spread showing that multipaths arrive from many different directions. Outdoor 140 GHz measurements [37] report up to 54° azimuth spread.

4) Small-scale fading models: In addition to delay and angular spreads, multipath cluster models are essential for proper characterization of small-scale fading of wave propagation channels. The number of clusters is up to 6 according to indoor office measurements [23], [33]. Intra-cluster azimuth spreads vary for measurements, probably because of differences in the resolution of sounders and clustering method. Intra-cluster azimuth spreads are up to 18° in indoor and outdoor channels [23], [33], [37]. Finally, small-scale fading of LOS omni-directional 140 GHz indoor channels is reported in [38] where the Nakagami-m distribution describes the measurement best.

5) Frequency dependency: Finally, variation of the studied channel parameters across radio frequencies would be our interest when extending the existing channel models for above-100 GHz RF. Comparisons of angular profiles of indoor multipath propagation at different RF, including below- and above-100 GHz [21], [24] report consistency of its spectrum shape across the tested RF because peaks corresponding to strong specular multipaths are found at similar angles. Papers comparing 28 and 140 GHz bands show a number of insights. For example, Nguyen *et al.* reports that the delay and angular spreads and cluster parameters at the two frequencies are similar in a large indoor hotspot, while Ju *et al.* [33] reports differences of delay spread and cluster angular spread between the two RF in an indoor office. The channel model by 3GPP [39] includes several frequency-dependent models of large-scale parameters, e.g., pathloss, delay and azimuth angular spreads. They are defined up to 86 GHz, but a recent paper [34] shows that the models fit measured large-scale parameters at 140 GHz well for indoor hotspots.

III. Hexa-X measurements

The literature survey in Section II indicates clear lack of channel model parameters covering different scenarios. It is attributed to a limited number of measurement campaigns. Hexa-X therefore focuses on performing measurements of above-100 GHz wave propagation as preparation to develop channel models.

A. Channel sounding

1) Bidirectional multipath measurements: A network analyzer and directive antennas together with rotating devices at both transmitter and receiver ends enable capturing bidirectional delay profiles of the propagation channel. The University of Oulu has a measurement system that is composed of Keysight PNA-X four-port network analyzer, Virgiania Diodes (VDI) frequency extenders, standard gain horn antennas, and three axis rotation units. Vector network analyzer (VNA) ports 1 and 3 are connected to the Tx extender and ports 2 and 4 to the Rx extender. Ports 1 and 2 operates at fixed frequency of 279 MHz and ports 3 and 4 sweeps the local oscillator from around 9.16 to 13.74 GHz. The RF, e.g., from 220 GHz to 330 GHz is swept at the Tx extender output and Rx extender input. The gain and half power beam width (HPBW) of horn antennas varies across frequency, being 20 dB and 18° at 250 GHz, respectively. The HPBW can be narrowed, and consequently the gain and angular resolution increased, by using lenses in addition to horns. Frequency extenders and horn antennas are available in Oulu for RFs 110–170, 140–220, and 220–330 GHz.

Bidirectional measurements become very slow when all rotation angle combinations of both antennas are considered. Especially, if both azimuth and elevation rotations are performed, the number of combinations grows with exponent of four. Moreover, if 2×2 polarization combinations are included, the number of frequency sweeps further quadruples. Even if a single frequency sweep of VNA is short and rotation motors are fast, the overall measurement time per location can easily increase to tens of hours. Such measurements evidently require static environment and do not enable motion of link ends.

Bidirectional measurements with wide bandwidth and consequently high delay resolution provide detailed information of the multipath structure. Together with a knowledge of the layout of measurement environment the tracing of paths may be supported. Common channel model parameters, such as angular spreads at both link ends, delays spreads etc. can be extracted.

2) Dynamic channel sounding at 140 GHz: The available amount of channel data at above-100 GHz is not large enough for physical layer simulations, partly because of the limited sounder capability. For example, as discussed in Section I, there seems to be no option of electrical steering of antenna beams yet for the frequency band. It is therefore necessary to rely on mechanical scanning of a directional antenna, which requires time to complete a measurement especially in double-directional sounding as detailed in Section III-A1). As a possible alternative, a continuous measurement of sectored omni-directional channels is studied in an effort to obtain *spatial scatterer distribution map* in a small cell scenario, instead of double-directional power angular profiles, using a principle of radar imaging, e.g., [40].

Continuous measurements of omni-directional channels is feasible by an ordinal real-time channel sounder. Two ultrawideband software defined radio peripherals of bandwidth greater than 2 GHz are integrated with frequency converters to produce RF at 140 GHz as illustrated in Fig. 1. A frequency-sweeping chirp signal is continuously transmitted from the base station (BS) and the receive waveform is recorded at the mobile station (MS) for post-processing the channel estimate. The frequency converters are equipped with $\times12$ frequency multiplier for local oscillator (LO) signals, which are mixed with the intermediate frequency (IF) signals from the transceivers. An open-waveguide probe is introduced at the sectored BS, while an omni-directional bicone antenna is used on the MS. Two RF amplifiers are integrated to increase the equivalent isotropic radiated power, which presently is limited to 22.5 dBm. Channel sounding consists of continuous acquisition of channel estimates during the MS travels along predefined routes. A link budget analysis shows that the sounder has a dynamic range of 115 dB, which is enough for a link up to 10 m link distance.

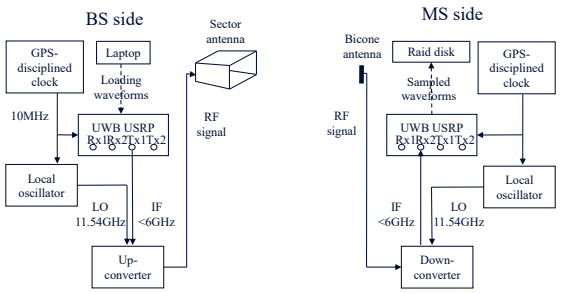

Fig. 1. Schematic of a dynamic mobile channel sounder at 140 GHz.

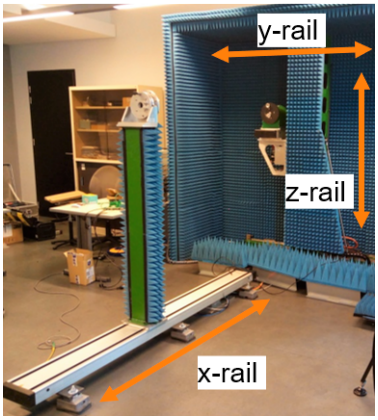

Fig. 2. Orange's measurement system for investigating wave–material interactions.

B. Wave–material interaction measurements

Orange has VNA-based systems covering continuously frequencies from a few GHz to 260 GHz. Channels from a few GHz to 50 GHz are characterized by a Keysight PNA-60 network analyser whereas frequencies from 50 GHz are characterized by a Rohde & Schwarz ZVA-40 network analyser and frequency extenders. OML extenders cover frequencies from 50-75 GHz and 75-110 GHz, VDI extenders covers frequencies from 110-170 GHz and 170 GHz-260 GHz. Antenna gains depend on frequencies and range from 13 dB to 25 dB. Frequency extenders are connected to the VNA similarly to the setup detailed in Section III-A1). Antennas or frequency extenders are set to linear rail mechanical units. One antenna can move along an horizontal axis x and the other antenna can move on a vertical y-z plane as illustrated in Fig. 2. When transmitter (Tx) and receiver (Rx) antennas are aligned and a material plate parallel to the y-z plane is inserted between antennas, reflection and transmission coefficients are collected at a normal incidence to the material. Different usual materials (glass, wood, plasterboard, etc) or potential obstacles (human body, vegetation, water bottles, etc) can be characterized continuously from a few GHz to 260 GHz making possible extensions from currently available material parameters.

Measurements in the University of Oulu use TeraPulse time domain spectroscopy platform that covers a wide RF from 100 GHz up to 1-2 THz for short-range atmospheric attenuation, transmission, reflection, and scattering measurements. The measurement distance is only a few tens of

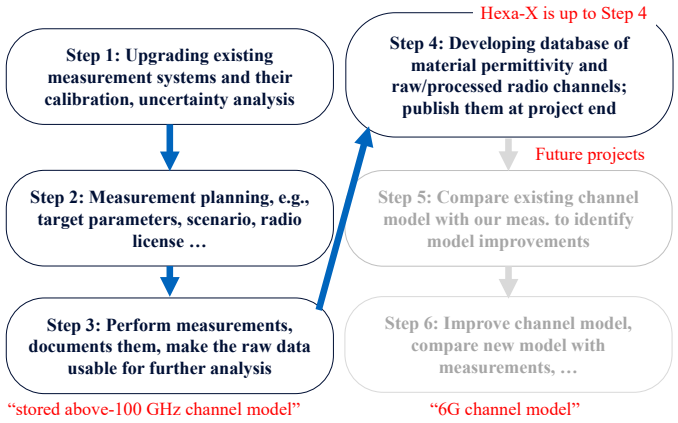

Fig. 3. Contributions of Hexa-X for 6G channel development.

centimetres. The transmitter radiates a collimated pulse that can be directed to either penetrate through or reflect/scatter from a slab of material sample or an object. The receiver samples the propagated impulse in the time domain using a high sampling rate. A frequency response of the signal propagation is then derived using the Fourier transformation. The measurement system can be used for many purposes, e.g., for determining directional scattering patterns, reflection and scattering power ratios, and transmission losses of different object on the wide RF range. The complex impulse response of reflected or transmitted wave is also used to determine material parameters like the permittivity and conductivity. There are various methods to extract these parameters, e.g., fitting measured reflection coefficients to the Fresnel equations [41]. The parameters can be used in many geometric channel models and especially in the ray tracing. Finally, the University of Oulu is also planning to build a measurement system for analyzing propagation effects due to water droplets of different size and density.

IV. Summary: Hexa-X Contribution to 6G Channel Model Development

As a summary of this paper, this section covers contributions of Hexa-X to channel models for above-100 GHz RF, i.e., development of a stored channel model and database of material permittivity for above-100 GHz, as illustrated in Fig. 3.

The use of measured channel responses for physical layer design and evaluation on a computer has been a well-recognized approach, e.g., [42], [43], as it allows repeatable tests and comparison of physical layer schemes. The fact that measured channel responses serve as the ground-truth of any simulation-based channel modelling also justifies the use for realistic evaluation of any radio systems. There are, however, also several drawbacks of using measured channels for physical layer studies, i.e., 1) measurements are always subject to uncertainties; 2) it is not straightforward to apply the measured channel responses to simulations that assume different hardware requirement than the measurement, e.g., signal dynamic range, antennas/arrays, system bandwidth and moving speed of a mobile; 3) a sufficient amount of measurements, e.g., for Monte-Carlo simulations and evaluation of packet error rates, may not be available due to limited capability of

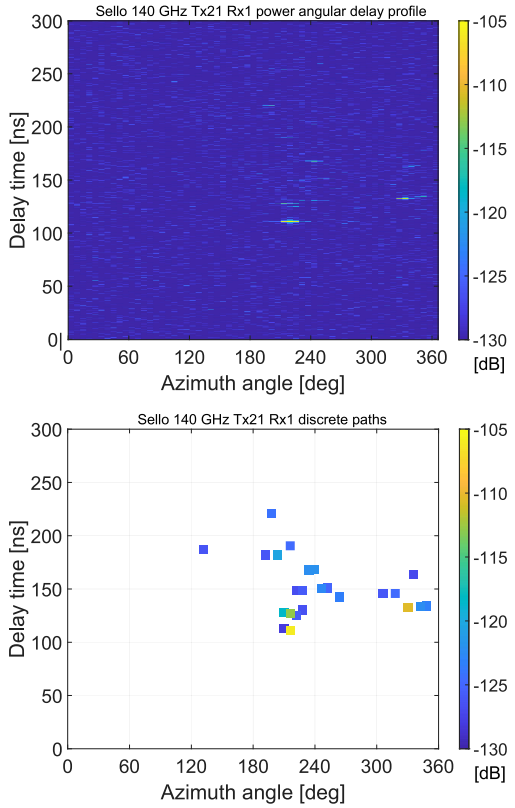

Fig. 4. (a) Band- and aperture-limited channel response from a measurement and (b) its band- and aperture-unlimited model as propagation paths. Data are from a shopping mall measurement at 140 GHz [23].

channel sounding. There are ways to overcome the mentioned drawbacks by, e.g., i) properly performing calibration of the channel sounder and filtering noise from measured channels, ii) under-sampling or interpolating the measured channels in space, bandwidth and time and iii) by making a general mathematical framework that allows us to over-sample or extrapolate the measured reality, which is called *a channel model*. The approach ii) is exemplified by Molisch *et al.* [42] where *band-/aperture-/time-sampling-limited* measurements of channels are approximated by the *band-/aperture-/time-sampling-unlimited* form. The former, coming from calibrated measurements, is represented by *power spectrum* while the latter is a discrete model of *propagation paths* represented by Dirac delta functions. Figure 4 illustrates the band-/aperture-limited and band-/aperture-unlimited forms of 140 GHz indoor channels. It is possible to reproduce *infinite* amount of small-scale fading realizations from the propagation paths of channels by applying the *uniform randomly distributed phases* to each path before summing them up at the antenna. The uniformly distributed phase variation to each path is justified by *a random local movement of a mobile terminal*. The exact paper [42] analyzes the Ergodic channel capacity of MIMO channels from limited MIMO channel sounding, whereas Selimis *et al.* [38] uses the same approach to identify the most suitable fading distribution at 140 GHz.

In Hexa-X, as a preparation to develop a channel model, i.e., the approach iii) mentioned in the previous paragraph, we aim at concentrating approaches i) and ii) that form foundation to realizing iii). The collection of propagation paths from measurements is called a *stored channel model*. The stored channel model, in the most complete set, will contain impulse responses

$$h(x_2, x_1, \Omega_2, \Omega_1, \tau, p_2, p_1) \in \mathbb{C}, \tag{1}$$

where x_2, x_1, Ω_2, Ω_1, τ, p_2, p_1 denote discrete Rx and Tx locations, angles of arrival and departure, propagation delay, and Rx and Tx polarizations, respectively. Our goal is to establish an extensive stored channel model and to open them as an asset of the public as was already practiced, though in a limited scale, by partly the same authors for 5 GHz MIMO channel sounding [44].

Acknowledgment

This work has been partly funded by the European Commission through the H2020 project Hexa-X (Grant Agreement no. 101015956) and partly by 6G Flagship programme, funded by Academy of Finland (grant no. 318927).

References

[1] M. Latva-aho and K. Leppänen (eds.), "Key drivers and research challenges for 6G ubiquitous wireless intelligence," White paper, September 2019.

[2] T. Tuovinen, N. Tervo, and A. Pärssinen, "Analyzing 5G RF system performance and relation to link budget for directive MIMO," *IEEE Transactions on Antennas and Propagation*, vol. 65, no. 12, pp. 6636–6645, 2017.

[3] ITU-R, "Effects of building materials and structures on radiowave propagation above about 100 mhz," Recommendation ITU-R P.2040-1, July 2015.

[4] R. Piesiewicz, C. Jansen, D. Mittleman, T. Kleine-Ostmann, M. Koch, and T. Kürner, "Scattering analysis for the modeling of THz communication systems," *IEEE Trans. Ant. Prop.*, vol. 55, no. 11, pp. 3002–3009, 2007.

[5] C. Jansen, R. Piesiewicz, D. Mittleman, T. Kürner, and M. Koch, "The impact of reflections from stratified building materials on the wave propagation in future indoor terahertz communication systems," *IEEE Trans. Ant. Prop.*, vol. 56, no. 5, pp. 1413–1419, 2008.

[6] C. Jansen, S. Priebe, C. Moller, M. Jacob, H. Dierke, M. Koch, and T. Kürner, "Diffuse scattering from rough surfaces in THz communication channels," *IEEE Trans. Terahertz Sci. Tech.*, vol. 1, no. 2, pp. 462–472, 2011.

[7] T. S. Rappaport, Y. Xing, O. Kanhere, S. Ju, A. Madanayake, S. Mandal, A. Alkhateeb, and G. C. Trichopoulos, "Wireless communications and applications above 100 GHz: Opportunities and challenges for 6G and beyond," *IEEE Access*, vol. 7, pp. 78 729–78 757, 2019.

[8] J. Ma, R. Shrestha, W. Zhang, L. Moeller, and D. M. Mittleman, "Terahertz wireless links using diffuse scattering from rough surfaces," *IEEE Trans. Terahertz Sci. Tech.*, vol. 9, no. 5, pp. 463–470, 2019.

[9] J. Kokkoniemi, J. Lehtomäki, and M. Juntti, "Measurements on penetration loss in terahertz band," in *Proc. 10th European Conf. Ant. Prop. (EuCAP 2016)*, 2016, pp. 1–5.

[10] J. Kokkoniemi, J. Lehtomäki, V. Petrov, D. Moltchanov, and M. Juntti, "Frequency domain penetration loss in the terahertz band," in *Proc. 2016 Global Symp. Millimeter Waves (GSMM) and ESA Works. Millimetre-Wave Tech. Appl.*, 2016, pp. 1–4.

[11] Y. Xing and T. S. Rappaport, "Propagation measurement system and approach at 140 GHz-moving to 6G and above 100 GHz," in *Proc. 2018 IEEE Global Commun. Conf. (GLOBECOM)*, 2018, pp. 1–6.

[12] V. Petrov, J. M. Eckhardt, D. Moltchanov, Y. Koucheryavy, and T. Kürner, "Measurements of reflection and penetration losses in low terahertz band vehicular communications," in *Proc. 14th European Conf. Ant. Prop. (EuCAP 2020)*, 2020, pp. 1–5.

[13] R. Piesiewicz, C. Jansen, S. Wietzke, D. Mittleman, M. Koch, and T. Kürner, "Properties of building and plastic materials in the THz range," *International Journal of Infrared and Millimeter Waves*, vol. 28, pp. 363–371, 2007.

[14] N. A. Abbasi, A. F. Molisch, and J. C. Zhang, "Measurement of directionally resolved radar cross section of human body for 140 and 220 GHz bands," in *Proc. 2020 IEEE Wireless Commun. Networ. Conf. Works. (WCNCW)*, 2020, pp. 1–4.

[15] I. Gordon, L. Rothman, C. Hill, and et al., "The hitran 2016 molecular spectroscopic database," Journal of Quantitative Spectroscopy and Radiative Transfer, pp. 3–69, December 2017.

[16] Terranova, "Channel and propagation modelling and characterization," project Deliverable D3.2, August 2018.

[17] ITU-R, "Specific attenuation model for rain for use in prediction methods," Recommendation ITU-R P.838-3, March 2005.

[18] ——, "Attenuation due to clouds and fogs," Recommendation ITU-R P.840-7, December 2017.

[19] S. Priebe, C. Jastrow, M. Jacob, T. Kleine-Ostmann, T. Schrader, and T. Kürner, "Channel and propagation measurements at 300 GHz," *IEEE Trans. Ant. Prop.*, vol. 59, no. 5, pp. 1688–1698, 2011.

[20] S. Kim, W. T. Khan, A. Zajić, and J. Papapolymerou, "D-band channel measurements and characterization for indoor applications," *IEEE Trans. Ant. Prop.*, vol. 63, no. 7, pp. 3198–3207, 2015.

[21] Bile Peng, S. Rey, and T. Kürner, "Channel characteristics study for future indoor millimeter and submillimeter wireless communications," in *Proc. 2016 10th European Conf. Ant. Prop. (EuCAP 2016)*, 2016, pp. 1–5.

[22] C. Cheng, S. Kim, and A. Zajić, "Comparison of path loss models for indoor 30 GHz, 140 GHz, and 300 GHz channels," in *Proc. 2017 11th European Conf. Ant. Prop. (EuCAP 2017)*, 2017, pp. 716–720.

[23] S. L. H. Nguyen, J. Järveläinen, A. Karttunen, K. Haneda, and J. Putkonen, "Comparing radio propagation channels between 28 and 140 GHz bands in a shopping mall," in *Proc. 12th European Conf. Ant. Prop. (EuCAP 2018)*, London, UK, 2018, pp. 1–5.

[24] E. M. Vitucci, M. Zoli, F. Fuschini, M. Barbiroli, V. Degli-Esposti, K. Guan, B. Peng, and T. Kürner, "Tri-band Mm-wave directional channel measurements in indoor environment," in *Proc. 2018 IEEE 29th Annual Int. Symp. Personal, Indoor Mobile Radio Commun. (PIMRC 2018)*, Bologna, Italy, 2018, pp. 205–209.

[25] L. Pometcu and R. D'Errico, "Channel model characteristics in D-band for NLOS indoor scenarios," in *Proc. 2019 13th European Conf. Ant. Prop. (EuCAP 2019)*, Krakow, Poland, 2019, pp. 1–4.

[26] C. Cheng, S. Sangodoyin, and A. Zajić, "THz MIMO channel characterization for wireless data center-like environment," in *Proc. 2019 IEEE Int. Symp. Ant. Prop. USNC-URSI Radio Sci. Meeting*, 2019, pp. 2145–2146.

[27] K. Guan, B. Peng, D. He, J. M. Eckhardt, S. Rey, B. Ai, Z. Zhong, and T. Kürner, "Measurement, simulation, and characterization of train-to-infrastructure inside-station channel at the terahertz band," *IEEE Trans. Terahertz Sci. Tech.*, vol. 9, no. 3, pp. 291–306, 2019.

[28] Y. Xing, O. Kanhere, S. Ju, and T. S. Rappaport, "Indoor wireless channel properties at millimeter wave and sub-Terahertz frequencies," in *Proc. 2019 IEEE Global Commun. Conf. (GLOBECOM '19)*, 2019, pp. 1–6.

[29] C. Cheng and A. Zajić, "Characterization of propagation phenomena relevant for 300 GHz wireless data center links," *IEEE Trans. Ant. Prop.*, vol. 68, no. 2, pp. 1074–1087, 2020.

[30] C. Cheng, S. Sangodoyin, and A. Zajić, "THz cluster-based modeling and propagation characterization in a data center environment," *IEEE Access*, vol. 8, pp. 56 544–56 558, 2020.

[31] D. Dupleich, R. Müller, S. Skoblikov, M. Landmann, G. D. Galdo, and R. Thomä, "Characterization of the propagation channel in conference room scenario at 190 GHz," in *Proc. 2020 14th European Conf. Ant. Prop. (EuCAP 2020)*, 2020, pp. 1–5.

[32] N. A. Abbasi, A. Hariharan, A. M. Nair, and A. F. Molisch, "Channel measurements and path loss modeling for indoor THz communication," in *Proc. 14th European Conf. Ant. Prop. (EuCAP2020)*, Copenhagen, Denmark, 2020, pp. 1–5.

[33] S. Ju, Y. Xing, O. Kanhere, and T. Rappaport, "3-D statistical indoor channel model for millimeter-wave and sub-Terahertz bands," in *Proc. 2020 IEEE Global Commun. Conf. (Globecom 2020)*, 2020, pp. 1–6. [Online]. Available: https://arxiv.org/abs/2009.12971

[34] S. L. H. Nguyen, K. Haneda, J. Järveläinen, A. Karttunen, and J. Putkonen, "Comparing radio propagation channels between 28 and 140 GHz bands in a shopping mall," in *Proc. 2021 IEEE 93rd Veh. Tech. COnf. (VTC2021-Spring)*, Helsinki, Finland, 2021. [Online]. Available: https://arxiv.org/abs/2009.13209

[35] J. M. Eckhardt, T. Doeker, S. Rey, and T. Kürner, "Measurements in a real data centre at 300 GHz and recent results," in *Proc. 2019 13th European Conf. Ant. Prop. (EuCAP 2019)*, 2019, pp. 1–5.

[36] S. Kim and A. G. Zajić, "Statistical characterization of 300-GHz propagation on a desktop," *IEEE Trans. Veh. Tech.*, vol. 64, no. 8, pp. 3330–3338, 2015.

[37] N. A. Abbasi, A. Hariharan, A. M. Nair, A. S. Almaiman, F. B. Rottenberg, A. E. Willner, and A. F. Molisch, "Double directional channel measurements for THz communications in an urban environment," in *Proc. 2020 IEEE Int. Conf. Commun. (ICC 2020)*, 2020, pp. 1–6. [Online]. Available: https://arxiv.org/abs/1910.01381

[38] D. Selimis, K. Ntontin, F. Lazarakis, and K. Haneda, "Initial investigation of D-band small-scale fading statistics," in *Proc. 2021 15th European Conf. Ant. Prop. (EuCAP 2021)*, 2021, pp. 1–5.

[39] 3GPP, "3GPP TR 38.901 v14.3.0: Study on channel model for frequencies from 0.5 to 100 GHz," Dec. 2017.

[40] K. Haneda, K. Takizawa, M. Kyrö, H. Hagiwara, and P. Vainikainen, "Scatterer localization in hospital rooms at 60 GHz," in *Proc. 2012 6th European Conf. Ant. Prop. (EuCAP 2012)*, Prague, Czech Republic, Apr. 2012, pp. 530–534.

[41] R. Piesiewicz, T. Kleine-Ostmann, N. Krumbholz, D. Mittleman, M. Koch, and T. Kürner, "Terahertz characterisation of building materials," *IET Electronics Letters*, vol. 41, no. 18, pp. 1002–1004, September 2005.

[42] A. F. Molisch, M. Steinbauer, M. Toeltsch, E. Bonek, and R. S. Thomä, "Capacity of MIMO systems based on measured wireless channels," *IEEE J. Sel. Areas Commun.*, vol. 20, no. 3, pp. 561–569, 2002.

[43] K. Kansanen, C. Schneider, T. Matsumoto, and R. Thomä, "Multilevel-coded QAM with MIMO turbo-equalization in broadband single-carrier signaling," *IEEE Trans. Veh. Tech.*, vol. 54, no. 3, pp. 954–966, 2005.

[44] C. Icheln and K. Haneda, "Plane-wave propagation path data from wideband MIMO channel sounding in an urban microcellular scenario," Mar. 2019. [Online]. Available: https://zenodo.org/record/2579734